
¹⁸F-FET PET Uptake Characteristics in Patients with Newly Diagnosed and Untreated Brain Metastasis

Marcus Unterrainer¹, Norbert Galldiks^{2,3}, Bogdana Suchorska⁴, Lara-Caroline Kowalew¹, Vera Wenter¹, Christine Schmid-Tannwald⁵, Maximilian Niyazi^{6,7}, Peter Bartenstein¹, Karl-Josef Langen^{2,8,9}, and Nathalie L. Albert¹

¹Department of Nuclear Medicine, University of Munich (LMU), Munich, Germany; ²Institute of Neuroscience and Medicine, Research Center Juelich, Juelich, Germany; ³Department of Neurology, University Hospital Cologne, Cologne, Germany; ⁴Department of Neurosurgery, LMU, Munich, Germany; ⁵Institute for Clinical Radiology, LMU, Munich, Germany; ⁶Department of Radiation Oncology, LMU, Munich, Germany; ⁷German Cancer Consortium (DKTK) & German Cancer Research Center (DKFZ), Heidelberg, Germany; ⁸Department of Nuclear Medicine, University of Aachen, Aachen, Germany; and ⁹JARA-Brain Section, Juelich-Aachen-Research-Alliance (JARA), Juelich, Germany

In patients with brain metastasis, PET using labeled amino acids has gained clinical importance, mainly regarding the differentiation of viable tumor tissue from treatment-related effects. However, there is still limited knowledge concerning the uptake characteristics in patients with newly diagnosed and untreated brain metastases. Hence, we evaluated the uptake characteristics in these patients using dynamic O-(2-¹⁸F-fluoroethyl)-L-tyrosine (¹⁸F-FET) PET. **Methods:** Patients with newly diagnosed brain metastases without prior local therapy and ¹⁸F-FET PET scanning were retrospectively identified in 2 centers. Static and dynamic PET parameters (maximal/mean tumor-to-brain-ratio [TBR_{max}/TBR_{mean}], biologic tumor volume [BTV], and time-activity curves with minimal time to peak [TTP_{min}]) were evaluated and correlated with MRI parameters (maximal lesion diameter, volume of contrast enhancement) and originating primary tumor. **Results:** Forty-five brain metastases in 30 patients were included. Forty of 45 metastases (89%) had a TBR_{max} ≥ 1.6 and were classified as ¹⁸F-FET-positive (median TBR_{max}, 2.53 [range, 1.64–9.47]; TBR_{mean}, 1.86 [range, 1.63–5.48]; and BTV, 3.59 mL [range, 0.04–23.98 mL], respectively). In 39 of 45 brain metastases eligible for dynamic analysis, a wide range of TTP_{min} was observed (median, 22.5 min; range, 4.5–47.5 min). All ¹⁸F-FET-negative metastases had a diameter of ≤ 1.0 cm, whereas metastases with a > 1.0 cm diameter all showed pathologic ¹⁸F-FET uptake, which did not correlate with lesion size. The highest variability of uptake intensity was observed within the group of melanoma metastases. **Conclusion:** Untreated metastases predominantly show increased ¹⁸F-FET uptake, and only a third of metastases < 1.0 cm were ¹⁸F-FET-negative, most likely because of scanner resolution and partial-volume effects. In metastases > 1.0 cm, ¹⁸F-FET uptake intensity was highly variable and independent of tumor size (even intraindividually). ¹⁸F-FET PET might provide additional information beyond the tumor extent by reflecting molecular features of a metastasis and might be a useful tool for future clinical applications, for example, response assessment.

Key Words: brain metastasis; ¹⁸F-FET PET; kinetic analysis

J Nucl Med 2017; 58:584–589

DOI: 10.2967/jnumed.116.180075

Brain metastases are secondary intracerebral neoplasms and occur in up to 17% of all cancer patients. Because of the improved treatment options for extracranial primary tumors with consecutive prolonged survival, the incidence of brain metastases is expected to increase. The most common originating primary tumors are lung cancer, breast cancer, and malignant melanoma (in sum up to 80% of all metastases) (1).

Systemic treatment usually consists of chemotherapy, immunotherapies, and targeted therapy, which, however, are mostly unable to cross the blood-brain barrier (BBB) (2,3). In brain metastases, treatment options such as whole resection, whole-brain radiation therapy, external fractionated radiotherapy, radiosurgery, and brachytherapy (4,5) are frequently used; additionally, recent experimental developments are heading toward new immunotherapies being able to cross the BBB (6).

Currently, contrast-enhanced standard MRI represents the diagnostic gold standard in the clinical management of patients with brain metastases (7). However, the diagnostic performance of this technique is limited regarding the differentiation between primary and secondary intracerebral malignancies, tumor delineation, differentiation of recurrent brain metastasis from posttherapeutic effects, and providing prognostic information in newly diagnosed brain tumors (8,9). Thus, there is an increasing demand for additional imaging options.

Regarding the diagnostic evaluation of intracerebral neoplasms, molecular imaging using PET has gained great importance. Particularly, radiolabeled amino acids such as O-(2-¹⁸F-fluoroethyl)-L-tyrosine (¹⁸F-FET) were reported to be particularly useful in glioma patients, for example, for biopsy guidance, planning of surgery and radiotherapy (10–12), as well as in secondary neoplasms for the differentiation between treatment-related changes from viable tumoral tissue (13). Furthermore, patterns of time-activity-curves and minimal time-to-peak (TTP_{min}) values derived from dynamic ¹⁸F-FET PET provide more detailed information on glioma characteristics. For example, it has been demonstrated that dynamic ¹⁸F-FET PET parameters have a high prognostic value in newly diagnosed low- and high-grade glioma (14,15). In secondary cerebral neoplasms, a few PET studies on pretreated brain metastases are currently available and have assessed the value of amino acid PET for the differentiation of recurrent disease from radiation-induced changes after radiotherapy (13,16–19). A recent study compared the tumor volume of partly untreated brain

Received Jun. 30, 2016; revision accepted Sep. 12, 2016.
For correspondence or reprints contact: Nathalie L. Albert, Department of Nuclear Medicine, LMU, Marchioninistrasse 15, 81377 Munich, Germany.
E-mail: nathalie.albert@med.uni-muenchen.de
Published online Oct. 6, 2016.
COPYRIGHT © 2017 by the Society of Nuclear Medicine and Molecular Imaging.

metastases in ^{18}F -FET PET and MRI, but there were criticisms regarding the methodology of that study (20,21). Up to now, no dynamic ^{18}F -FET PET study has evaluated the uptake characteristics of brain metastases at initial diagnosis before local treatment. Thus, we analyzed characteristics of newly diagnosed and untreated brain metastases using static and dynamic ^{18}F -FET PET with respect to the originating primary tumor.

MATERIALS AND METHODS

Patients

Patients with brain metastases and available ^{18}F -FET PET examination between the years 2008 and 2015 at the University of Munich, Munich, Germany (LMU), and Research Center Juelich, Germany (FZJ), were retrospectively identified. All newly diagnosed metastases without prior local therapy (i.e., whole-brain radiation therapy, radio-surgery, external fractionated radiotherapy, brachytherapy, or resection) were included in the study. The study was approved by the ethical review board of the LMU. All patients gave written informed consent before each ^{18}F -FET PET investigation as part of the clinical routine.

PET Acquisition and Data Evaluation

Dynamic ^{18}F -FET PET scans were acquired with an ECAT Exact HR+ scanner (Siemens) at LMU and FZJ according to the standard protocols of both centers (22,23). Both static and dynamic ^{18}F -FET PET were evaluated on a Hermes workstation (Hermes Medical Solutions) as described previously (22). For the assessment of the maximal tumor-to-background ratio (TBR_{max}), the maximal SUV of the tumor was divided by the mean background activity in the healthy contralateral hemisphere. Furthermore, the biologic tumor volume (BTV) was estimated by semiautomatic calculation of a volume of interest using a threshold of $\text{TBR} \geq 1.6$, which has been proposed as an optimal threshold between tumor and surrounding healthy tissue (24). Accordingly, the mean tumor-to-background ratio (TBR_{mean}) was evaluated as the mean uptake within the BTV; when no BTV could be delineated because of ^{18}F -FET uptake below the threshold of 1.6, the TBR_{mean} was determined within a volume of interest based on the corresponding contrast enhancement in the spatially coregistered MRI.

As also described previously (25), dynamic PET data were evaluated according to standardized clinical procedures using the software PET Display Dynamic implemented in the Hermes workstation: the early summation images (10–30 min after injection) were used to generate a 90% isocontour region of interest, which was applied to the dynamic PET images to extract the time–activity curves slice by slice. Within 40 min after injection, a time–activity curve grading of all time–activity curves of each metastasis was performed according to the following classifications: solely increasing time–activity curves, predominantly increasing time–activity curves, mixed time–activity curve patterns, predominantly decreasing time–activity curves, and solely decreasing time–activity curves. Time–activity curve grades 1–2 were then classified as increasing time–activity curves and grades 3–5 as decreasing time–activity curves. Additionally, the TTP was assessed in each slice within the tumor and the shortest TTP in at least 2 consecutive slices was defined as TTP_{min} , as previously published (15). At the FZJ, dynamic ^{18}F -FET PET imaging was performed as described elsewhere (23).

MRI

Patients underwent routine MRI (1.5 T or 3 T) with a standard head coil before and after administration of a gadolinium-based contrast agent (T1- and T2-weighted). Axial T1-weighted images were obtained from the second cervical vertebral body to the vertex. The maximum diameter of the entire metastatic lesion including all contrast-enhancing areas ($\text{diameter}_{\text{ce}}$) was measured. Furthermore, to exclude cystic or necrotic tumor parts from the measurements, the volume of the contrast enhancement (VOL_{ce}) was evaluated by slice-by-slice volumetry by an

experienced radiologist. In 2 patients with 2 metastases, the evaluation of $\text{diameter}_{\text{ce}}$ and VOL_{ce} , however, was based on contrast-enhanced CT only. Because of the spatial resolution of the ECAT scanner, only metastases with a $\text{diameter}_{\text{ce}} > 0.5$ cm were included in the analysis.

Statistics

Statistical analysis was performed with SPSS Statistics (version 23; IBM). Descriptive statistics were used for patient characteristics and ^{18}F -FET PET data including the TTP_{min} , TBR_{max} , TBR_{mean} , BTV, $\text{diameter}_{\text{ce}}$, and VOL_{ce} . Normal distribution was assessed using the Shapiro–Wilk test. Spearman correlation was used to evaluate the correlations of TBR_{max} , TBR_{mean} , BTV, $\text{diameter}_{\text{ce}}$, and VOL_{ce} . Distributions between particular groups were evaluated using a χ^2 test. Continuous and not normally distributed parameters were compared using the Mann–Whitney-*U* test and Kruskal–Wallis test, respectively. Statistical significance was defined as 2-tailed *P* values below 0.05.

RESULTS

Patient Characteristics

Forty-five metastatic lesions in 30 patients (16 women; median age, 68.0 y; range, 17.0–86.0 y) were included in the study. Overall, 34 ^{18}F -FET PET scans were analyzed. Of those, 27 ^{18}F -FET PET scans were obtained between 2008 and 2015 at the Department of Nuclear Medicine, LMU, Munich, Germany, and 7 scans between 2008 and 2013 at the Institute of Neuroscience and Medicine, FZJ, Juelich, Germany. Fourteen of 30 patients had lung cancer (16 metastases), 4 patients breast cancer (5 metastases), and 10 patients malignant melanoma (22 metastases). Additionally, 1 patient had Ewing sarcoma and 1 a cancer of unknown primary (1 metastasis each) (Table 1). A histopathologic confirmation of the brain metastases was performed in 19 of 30 patients (63%) patients (12 patients at LMU and 7 patients at FZJ).

Twenty-five patients with 34 brain metastases did not receive any chemotherapy that was able to cross the BBB before the ^{18}F -FET PET scan. Concurrently or within 6 mo before ^{18}F -FET PET imaging, 5 patients with 11 metastatic lesions received chemotherapy that was able to cross the BBB (all included metastatic lesions are provided in Supplemental Table 1 [supplemental materials are available at <http://jnm.snmjournals.org>]).

Overall Static and Dynamic ^{18}F -FET PET and MRI Characteristics

All metastatic lesions showed contrast enhancement. Forty metastases (89%) were ^{18}F -FET–positive and had a $\text{TBR}_{\text{max}} \geq 1.6$ (median TBR_{max} , 2.53 and range, 1.64–9.47; median $\text{diameter}_{\text{ce}}$, 2.1 cm and range, 0.6–6.0 cm; median VOL_{ce} , 4.57 mL and range, 0.14–63.10 mL).

Five brain metastases (11%) had a $\text{TBR}_{\text{max}} < 1.6$ and were classified as ^{18}F -FET–negative (median TBR_{max} , 1.34; range, 1.25–1.50). All of them had a $\text{diameter}_{\text{ce}}$ of ≤ 1.0 cm (median, 0.8 cm and range, 0.7–1.0 cm; median VOL_{ce} , 0.18 mL and range, 0.05–0.93 mL). However, among all metastases with a $\text{diameter}_{\text{ce}}$ of ≤ 1.0 cm ($n = 14$), 9 metastases (64%) were ^{18}F -FET–positive (median TBR_{max} , 2.01; range, 1.78–7.35). Table 1 provides further specifications.

The analysis of the TBR_{mean} in ^{18}F -FET–positive metastases revealed a median value of 1.86 (range, 1.63–5.48). The median BTV in the overall group was 3.59 mL (range, 0.04–23.98 mL). Table 1 provides further specifications.

Thirty-nine metastases were eligible for the dynamic analysis. In the whole cohort, a wide range of TTP_{min} was observed (median, 22.5 min; range, 4.5–47.5 min; Fig. 1) as well as both increasing

TABLE 1
Overview of MRI and Static ¹⁸F-FET PET Parameters

Parameter	Overall (n = 45)	Lung cancer (n = 16)	Breast cancer (n = 5)	Melanoma (n = 22)	Ewing sarcoma (n = 1)	Cancer of unknown primary (n = 1)
Median diameter _{ce} (cm)	1.8	2.1	1.6	1.4	1.7	3.0
Range diameter _{ce} (cm)	0.6–6.0	0.8–6.0	0.7–2.4	0.6–5.0	—	—
Median VOL _{ce} (mL)	3.31	4.33	3.69	1.45	1.19	7.63
Range VOL _{ce} (mL)	0.05–63.10	0.22–63.10	0.22–9.08	0.05–15.95	—	—
¹⁸ F-FET-positive	40/45 (89%)	16/16 (100%)	4/5 (80%)	18/22 (82%)	1/1 (100%)	1/1 (100%)
Median TBR _{max}	2.53	2.61	2.97	2.20	4.01	1.8
Range TBR _{max}	1.64–9.47	1.64–5.10	2.12–3.11	1.66–9.47	—	—
Median TBR _{mean}	1.86	1.88	2.05	1.78	2.31	1.66
Range TBR _{mean}	1.63–5.48	1.64–2.67	1.79–2.19	1.63–5.48	—	—
Median BTV (mL)	3.59	5.11	6.46	1.25	5.62	0.48
Range BTV (mL)	0.04–23.98	0.06–22.85	0.36–23.98	0.04–10.95	—	—

and decreasing time–activity curves. Time–activity curves were increasing in 12 metastases and decreasing in 27 metastases throughout all pathologic subgroups.

In the subgroup of patients with multiple metastatic lesions (8 patients with 24 metastases), 4 patients showed concordant time–activity curves in the intraindividual multiple metastases, whereas 4 patients showed discordant time–activity curves. Additionally, the intraindividual metastases showed an identical TTP_{min} in only 3 patients, whereas in 5 patients the TTP_{min} differed considerably.

Static and Dynamic ¹⁸F-FET PET and MRI Characteristics in Relation to Primary Tumor

Four of 5 ¹⁸F-FET–negative metastases originated from malignant melanoma (median diameter_{ce}, 0.9 cm; range, 0.7–1.0 cm), no metastasis from lung cancer, and 1 metastasis from breast cancer (diameter_{ce}, 0.7 cm), respectively. However, there was no significantly different distribution of ¹⁸F-FET–negative metastases throughout the subgroups of originating entities (*P* = 0.186; Table 1 provides further specifications).

There was no significantly different median diameter_{ce} (*P* = 0.435), VOL_{ce} (*P* = 0.323), TBR_{max} (*P* = 0.572), TBR_{mean} (*P* = 0.534), or BTV (*P* = 0.520) among the 3 major groups of ¹⁸F-FET–positive metastases.

Lung cancer metastases exhibited high ¹⁸F-FET uptake even in small lesions of ≤ 1.0 cm (median TBR_{max}, 2.61 and range, 1.64–5.10; diameter_{ce}, 2.1 cm and range, 0.8–6.0 cm), which did not show any correlation with MRI metrics (TBR_{max} and diameter_{ce}, *R* = 0.246, *P* = 0.358; TBR_{max} and VOL_{ce}, *R* = 0.126, *P* = 0.641; Fig. 2 provides an example).

Malignant melanoma metastases had the highest variability of ¹⁸F-FET uptake, spanning a wide range of TBR_{max} values (1.25–9.47) with extraordinarily high individual uptake values (Fig. 3). Additionally, there was no significant correlation of TBR_{max} and VOL_{ce} (*R* = 0.189, *P* = 0.453) or TBR_{max} and diameter_{ce} (*R* = 0.051, *P* = 0.842) could be observed. In the case of breast cancer metastases, no correlation analyses were performed because of the small number of data points (*n* = 5).

In line with the correlations to TBR_{max}, the correlations of TBR_{mean} with the MRI parameters revealed results similar to those displayed in Table 2.

The MRI-derived volume VOL_{ce} showed a significant correlation with the PET-derived BTV (*R* = 0.630; *P* < 0.001) in the whole cohort as well as similar high correlations throughout the pathologic subgroups (Table 2).

For TTP_{min} in the dynamic evaluation, a wide range could be observed throughout the subgroups without particular tendency in the pathologic subgroups, but a high portion of cases with decreasing time–activity curves and early TTP_{min} throughout the whole cohort.

PET Findings in Relation to Chemotherapy Crossing BBB

In 8 ¹⁸F-FET–positive metastases, a systemic chemotherapy able to cross the BBB was administered concurrently or within

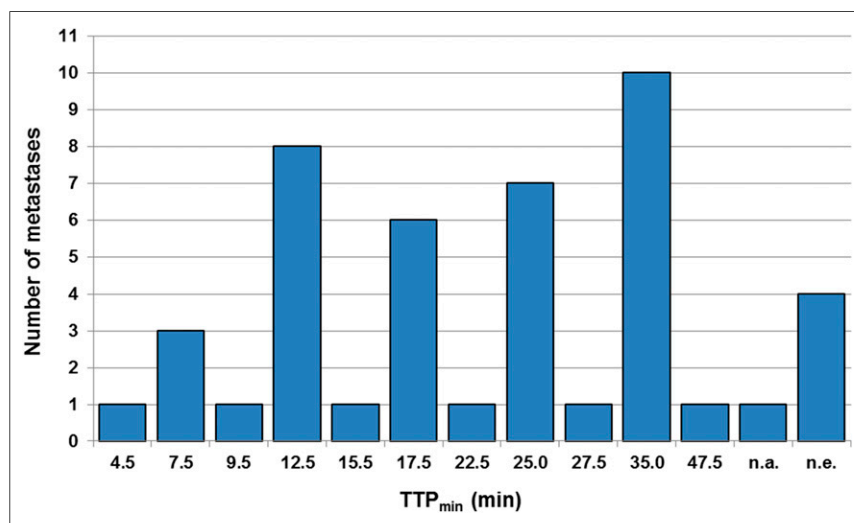


FIGURE 1. Distribution of TTP_{min} in metastases eligible for dynamic ¹⁸F-FET PET imaging. n.a. = not available; n.e. = not evaluable.

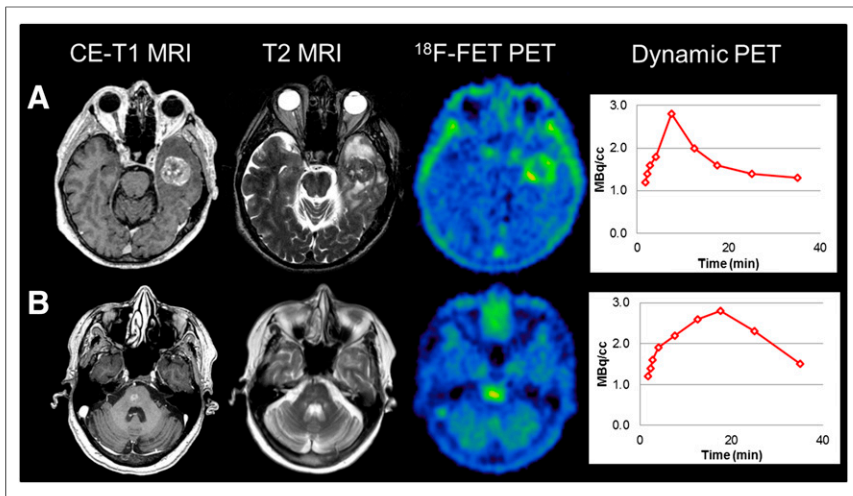


FIGURE 2. Two patients with metastatic lesions originating from lung cancer. (A) Diameter_{ce}: 3.6 cm, VOL_{ce}: 10.01 mL, TBR_{max}: 3.09, TBR_{mean}: 2.07, BTv: 7.68 mL, and decreasing time-activity curve (TTP_{min}, 7.5 min). (B) Diameter_{ce}: 0.8 cm, VOL_{ce}: 0.22 mL, TBR_{max}: 2.46, TBR_{mean}: 1.89, BTv: 2.11 mL, and decreasing time-activity curve (TTP_{min}, 17.5 min).

6 mo before the ¹⁸F-FET PET scans (32 without chemotherapy). Regarding the ¹⁸F-FET PET-derived parameters TBR_{max}, TBR_{mean}, and BTv as well as the VOL_{ce} and diameter_{ce}, a prior or concurrent chemotherapy did not have a significant impact on these parameters when compared with metastases without chemotherapy (Table 3). Furthermore, there was a heterogeneous distribution of time-activity curves and TTP_{min} throughout those 2 groups.

DISCUSSION

Although literature exists describing a high diagnostic accuracy of amino acid PET for the differentiation of viable tumor from treatment-related effects in pretreated brain metastases, there is only limited literature regarding the characteristics of newly diagnosed and untreated brain metastases using ¹⁸F-FET PET.

especially in tumors with low tracer uptake, rather than to a complete lack of ¹⁸F-FET uptake as observed in 30% of low-grade gliomas (14,26). This might especially be the case because a missing expression of the L-amino-acid transporter, responsible for ¹⁸F-FET uptake in brain metastases, was reported to be a rare condition itself (27). Therefore, pursuing the ¹⁸F-FET PET assessment of metastases with a diameter_{ce} of < 1.0 cm is of limited value, because a negative finding not necessarily excludes viable tumor.

In contrast to our study, Gempt et al. did not present any cases of ¹⁸F-FET-negative metastases—that is, all metastases were reported to provide a significant ¹⁸F-FET uptake (TBR > 1.6) (20). In the study by Gempt et al., however, the lesion size is not mentioned and it remains unclear whether very small lesions were included or the observed increased ¹⁸F-FET uptake in all metastases was caused by a selection bias—that is, well-delineated metastases with highly increased ¹⁸F-FET uptake eligible for neurosurgical resection might have been included in this retrospective study.

Although there was no tumor subtype in our study with a characteristic ¹⁸F-FET uptake that can be clearly distinguished from other subtypes, metastases originating from different primary tumors showed different uptake behavior. In our cohort, all metastases from lung cancer showed pathologic ¹⁸F-FET uptake, which was independent of the lesion size. Therefore, even small metastases with a ≤ 1.0-cm diameter_{ce} could easily be detected by increased ¹⁸F-FET uptake.

Interestingly, a high variability of uptake intensity could be observed within the group of metastatic lesions originating from malignant melanoma—that is, both smaller and larger metastases could show remarkably low as well as high TBR_{max} and TBR_{mean} values. In patients with multiple metastases derived from malignant

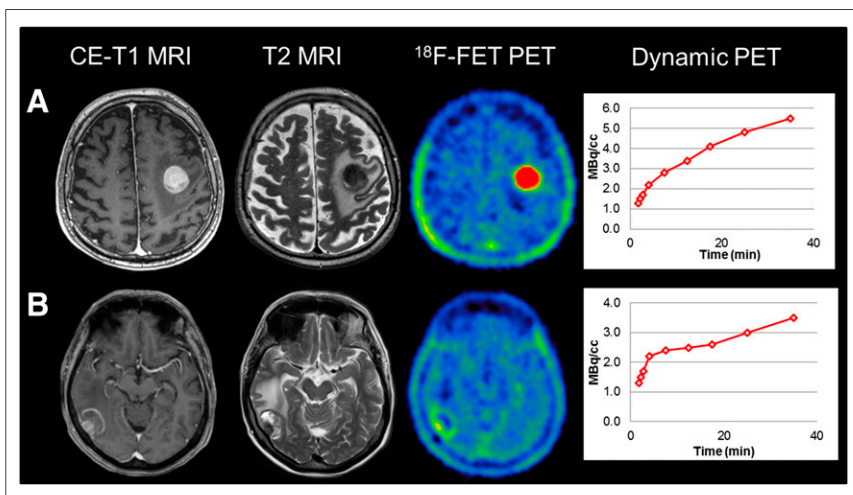


FIGURE 3. Two patients with metastatic lesions originating from malignant melanoma. (A) Diameter_{ce}: 2.8 cm, VOL_{ce}: 10.01 mL, TBR_{max}: 9.47, TBR_{mean}: 3.71, BTv: 10.95 mL, and increasing time-activity curve (TTP_{min}, 35 min). (B) Diameter_{ce} of entire metastatic lesion: 2.9 cm, VOL_{ce}: 5.08, TBR_{max}: 2.28, TBR_{mean}: 1.73, BTv: 3.27 mL, and increasing time-activity curve (TTP_{min}, 35 min).

TABLE 2
Correlation of MRI Metrics and PET Parameters of ¹⁸F-FET-Positive Metastases

Correlation parameter	Overall (n = 40) R	Lung cancer (n = 16) R	Melanoma (n = 18) R
TBR _{max} /diameter _{ce}	0.121 (0.457)	0.246 (0.358)	0.051 (0.842)
TBR _{mean} /diameter _{ce}	-0.043 (0.791)	-0.040 (0.884)	-0.065 (0.797)
BTV/diameter _{ce}	0.504 (0.001)	0.718 (0.002)	0.466 (0.052)
TBR _{max} /VOL _{ce}	0.168 (0.301)	0.126 (0.641)	0.189 (0.453)
TBR _{mean} /VOL _{ce}	0.020 (0.902)	-0.156 (0.564)	0.088 (0.729)
BTV/VOL _{ce}	0.630 (<0.001)	0.676 (0.004)	0.587 (0.010)

Data in parentheses are *P* values.

melanoma, this could even be observed intraindividually. This variable ¹⁸F-FET uptake might be attributed to different malignant melanoma metastasis subtypes, for example, amelanotic melanoma histology, which could not be assessed in all cases because of the missing histopathologic confirmation. Furthermore, general heterogeneity of brain metastases could be discussed as cause as well (28,29).

Regarding the dynamic ¹⁸F-FET PET evaluation, a broad distribution of time-activity curves and TTP_{min} throughout all metastatic subgroups could be observed, indicating that metastases of a particular primary tumor do not have specific characteristic patterns in dynamic ¹⁸F-FET PET, whereas, notably, a high portion of metastases throughout the entire cohort provided decreasing time-activity curves with early TTP_{min}. Whether dynamic PET parameters before further therapies do have a prognostic value at initial diagnosis, such as shown in primary gliomas (14,15), has to be evaluated in prospective settings. Additionally, all metastatic lesions showed time-activity curves characteristic for brain neoplasms, whereas no time-activity curve with a shape specific for vascular structures was seen. Although it is intriguing to speculate that the ¹⁸F-FET signal might be a result of higher blood volume in brain metastases due to, for example, neovascularization, the characteristic nonvascular time-activity curves renders a major impact of the blood volume on the tumoral ¹⁸F-FET uptake unlikely. Also a mere ¹⁸F-FET influx through the disrupted BBB can be excluded (30), because a BBB disruption is also seen in nontumorous lesions such as radionecrosis, but without pathologic ¹⁸F-FET uptake (16). Therefore, as in gliomas, tumoral ¹⁸F-FET uptake in metastases is also attributed to the L-amino-acid transporter (27).

A further interesting aspect is the comparison of ¹⁸F-FET parameters with the MRI metrics. Notably, in ¹⁸F-FET-positive me-

tastases there was no correlation of the ¹⁸F-FET uptake intensity (TBR_{max} and TBR_{mean}) with the maximal metastatic lesion diameter_{ce} as well as the VOL_{ce}. The volume of the contrast-enhancing tumor parts was included in our study, as the mere 1-dimensional metric information using the maximal diameter for brain metastases assessment is a controversial issue (7) because of the broad heterogeneity of morphologic appearance with regard to shape and structure of metastatic lesions. The proposed Revised Assessment in Neuro-Oncology criteria for brain metastases suggest a measurement of only solid tumor parts in 1 dimension, whereas cystic or necrotic metastases are defined as nonmeasurable lesions and therefore remain a particular challenge for morphologic imaging alone (7) and, consequently, for response assessment. Therefore, the volume of the contrast-enhancing tumor parts was suggested as a possibly more accurate assessment parameter for brain metastases (7,31). In our study, we could observe a significant correlation of VOL_{ce} and BTV throughout all groups under investigation (*R* = 0.630; *P* < 0.001) with a threshold of TBR ≥ 1.6, which was derived from glioma studies. Whether there is a specific threshold for the BTV estimation in secondary brain tumors needs to be evaluated in future combined PET and histopathology studies using stepwise biopsies. In contrast, there was no correlation of the ¹⁸F-FET uptake intensity with the VOL_{ce}; this suggests that the uptake intensity in ¹⁸F-FET PET represents an additional aspect beyond the tumoral extent of a metastatic lesion by possibly reflecting molecular features in terms of biologic tumor behavior, which cannot be assessed with mere morphologic imaging. Besides the well-known clinical value regarding the differentiation of viable tumor and treatment-related changes, these particular features might be of special interest for clinical applications in yet untreated metastatic lesions regarding prognostication as well as

TABLE 3
Influence of BBB-Crossing Chemotherapy on PET and MRI Parameters in ¹⁸F-FET-Positive Metastases

Correlation pair	TBR _{max}	TBR _{mean}	BTV (mL)	VOL _{ce} (mL)	Diameter _{ce} (cm)
BBB-crossing chemotherapy (n = 8)					
Median	3.38	2.08	4.65	2.14	1.7
Range	1.79–4.39	1.68–2.32	0.14–23.98	0.19–9.08	0.9–2.6
Non-BBB-crossing chemotherapy (n = 32)					
Median	2.37	1.82	2.09	4.57	2.2
Range	1.64–9.47	1.63–5.48	0.04–22.85	0.14–63.10	0.6–6.0
Mann-Whitney <i>U</i> test	<i>P</i> = 0.309	<i>P</i> = 0.197	<i>P</i> = 0.396	<i>P</i> = 0.359	<i>P</i> = 0.209

response assessment of brain metastases. These interesting aspects need to be addressed in future studies.

Additionally, some limitations of this study should be addressed. First, limitations arise from the retrospective study design. Second, although the same type of PET scanner was used in both participating sites, there are minor differences in the dynamic scanning protocol (e.g., different number of frames and frame durations). Nonetheless, both imaging protocols are in line with German and European Association of Nuclear Medicine guidelines for PET imaging of brain tumors (32,33). Third, histology of newly diagnosed brain metastases could not be obtained in all cases. It is desirable to validate ^{18}F -FET PET by histopathology, but because of a poor clinical condition or patient refusal, in a considerable number of patients histopathology could not be obtained, which is an intrinsic limitation of retrospective studies. The accuracy of diagnosis can be assumed because the included patients were with known extracranial tumors with—most likely—consecutive cerebral metastases during the course of the disease. In the single case of cancer of unknown primary, histology could be obtained. Fourth, the number of examined patients is relatively low, particularly the number of breast cancer metastases. On the other hand, this is up to now the largest study of newly diagnosed brain metastases.

CONCLUSION

Newly diagnosed and locally untreated brain metastases predominantly showed increased ^{18}F -FET uptake. Only a third of metastases ≤ 1.0 cm was ^{18}F -FET-negative, most likely because of the scanner resolution and partial-volume effects. In metastases > 1.0 cm, ^{18}F -FET uptake intensity showed a high variability independent of tumor size (even intraindividually), so that ^{18}F -FET PET might provide additional information reflecting biologic tumor behavior and molecular features beyond the morphologic tumor extent. New clinical applications of ^{18}F -FET PET as a complementary tool might arise for brain metastasis imaging.

DISCLOSURE

No potential conflict of interest relevant to this article was reported.

ACKNOWLEDGMENT

Parts of this study originate from the doctoral thesis of Lara-Caroline Kowalew.

REFERENCES

- Nayak L, Lee EQ, Wen PY. Epidemiology of brain metastases. *Curr Oncol Rep*. 2012;14:48–54.
- Crivellari D, Pagani O, Veronesi A, et al. High incidence of central nervous system involvement in patients with metastatic or locally advanced breast cancer treated with epirubicin and docetaxel. *Ann Oncol*. 2001;12:353–356.
- Bendell JC, Domchek SM, Burstein HJ, et al. Central nervous system metastases in women who receive trastuzumab-based therapy for metastatic breast carcinoma. *Cancer*. 2003;97:2972–2977.
- Kaal ECA, Niël CGJH, Vecht CJ. Therapeutic management of brain metastasis. *Lancet Neurol*. 2005;4:289–298.
- Lin X, DeAngelis LM. Treatment of brain metastases. *J Clin Oncol*. 2015;33:3475–3484.
- Rosell R, Karachaliou N. Trends in immunotherapy for brain metastases. *Lancet Oncol*. 2016;17:859–860.
- Lin NU, Lee EQ, Aoyama H, et al. Response assessment criteria for brain metastases: proposal from the RANO group. *Lancet Oncol*. 2015;16:e270–e278.
- Puhalla S, Elmquist W, Freyer D, et al. Unsantifying the sanctuary: challenges and opportunities with brain metastases. *Neuro-oncol*. 2015;17:639–651.
- Huang C, McConathy J. Radiolabeled amino acids for oncologic imaging. *J Nucl Med*. 2013;54:1007–1010.
- Niyazi M, Geisler J, Siefert A, et al. FET-PET for malignant glioma treatment planning. *Radiother Oncol*. 2011;99:44–48.
- Piroth MD, Pinkawa M, Holy R, et al. Integrated-boost IMRT or 3-D-CRT using FET-PET based auto-contoured target volume delineation for glioblastoma multiforme - a dosimetric comparison. *Radiat Oncol*. 2009;4:57.
- Wyss M, Hofer S, Bruehlmeier M, et al. Early metabolic responses in temozolomide treated low-grade glioma patients. *J Neurooncol*. 2009;95:87–93.
- Galldiks N, Stoffels G, Filss CP, et al. Role of O-(2- ^{18}F -fluoroethyl)-L-tyrosine PET for differentiation of local recurrent brain metastasis from radiation necrosis. *J Nucl Med*. 2012;53:1367–1374.
- Jansen NL, Suchorska B, Wenter V, et al. Dynamic ^{18}F -FET PET in newly diagnosed astrocytic low-grade glioma identifies high-risk patients. *J Nucl Med*. 2014;55:198–203.
- Jansen NL, Suchorska B, Wenter V, et al. Prognostic significance of dynamic ^{18}F -FET PET in newly diagnosed astrocytic high-grade glioma. *J Nucl Med*. 2015;56:9–15.
- Ceccon G, Lohmann P, Stoffels G, et al. Dynamic O-(2- ^{18}F -fluoroethyl)-L-tyrosine positron emission tomography differentiates brain metastasis recurrence from radiation injury after radiotherapy. *Neuro-oncol*. July 28, 2016 [Epub ahead of print].
- Lizarraga KJ, Allen-Auerbach M, Czernin J, et al. ^{18}F -FDOPA PET for differentiating recurrent or progressive brain metastatic tumors from late or delayed radiation injury after radiation treatment. *J Nucl Med*. 2014;55:30–36.
- Terakawa Y, Tsuyuguchi N, Iwai Y, et al. Diagnostic accuracy of ^{11}C -methionine PET for differentiation of recurrent brain tumors from radiation necrosis after radiotherapy. *J Nucl Med*. 2008;49:694–699.
- Grosu A-L, Astner ST, Riedel E, et al. An interindividual comparison of O-(2- ^{18}F -fluoroethyl)-L-tyrosine (FET) and L-[methyl- ^{11}C]-methionine (MET)-PET in patients with brain gliomas and metastases. *Int J Radiat Oncol Biol Phys*. 2011;81:1049–1058.
- Gempt J, Bette S, Buchmann N, et al. Volumetric analysis of F-18-FET-PET imaging for brain metastases. *World Neurosurg*. 2015;84:1790–1797.
- Langen K-J, Tonn JC, Albert NL, Galldiks N. Letter to the editor: comparing the volume of brain metastases in F-18-FET-PET and MR. *World Neurosurg*. 2016;89:722.
- Jansen NL, Graute V, Armbruster L, et al. MRI-suspected low-grade glioma: is there a need to perform dynamic FET PET? *Eur J Nucl Med Mol Imaging*. 2012;39:1021–1029.
- Galldiks N, Stoffels G, Filss C, et al. The use of dynamic O-(2- ^{18}F -fluoroethyl)-L-tyrosine PET in the diagnosis of patients with progressive and recurrent glioma. *Neuro-oncol*. 2015;17:1293–1300.
- Pauleit D, Floeth F, Hamacher K, et al. O-(2- ^{18}F -fluoroethyl)-L-tyrosine PET combined with MRI improves the diagnostic assessment of cerebral gliomas. *Brain*. 2005;128:678–687.
- Niyazi M, Jansen N, Ganswindt U, et al. Re-irradiation in recurrent malignant glioma: prognostic value of ^{18}F -FET-PET. *J Neurooncol*. 2012;110:389–395.
- Unterrainer M, Schweisthal F, Suchorska B, et al. Serial ^{18}F -FET PET imaging of primarily ^{18}F -FET-negative glioma: does it make sense? *J Nucl Med*. 2016;57:1177–1182.
- Papin-Michault C, Bonnetaud C, Dufour M, et al. Study of LAT1 expression in brain metastases: towards a better understanding of the results of positron emission tomography using amino acid tracers. *PLoS One*. 2016;11:e0157139.
- Berghoff A, Bago-Horvath Z, De Vries C, et al. Brain metastases free survival differs between breast cancer subtypes. *Br J Cancer*. 2012;106:440–446.
- Wilmott JS, Menzies AM, Haydu LE, et al. BRAFV600E protein expression and outcome from BRAF inhibitor treatment in BRAFV600E metastatic melanoma. *Br J Cancer*. 2013;108:924–931.
- Langen K-J, Galldiks N. Reply to “[^{18}F]-fluoro-ethyl-L-tyrosine PET: a valuable diagnostic tool in neuro-oncology, but not all that glitters is glioma” by Hutterer et al. *Neuro-oncol*. 2013;15:816–817.
- Bauknecht H-C, Romano VC, Rogalla P, et al. Intra- and interobserver variability of linear and volumetric measurements of brain metastases using contrast-enhanced magnetic resonance imaging. *Invest Radiol*. 2010;45:49–56.
- Langen K-J, Bartenstein P, Boecker H, et al. German guidelines for brain tumour imaging by PET and SPECT using labelled amino acids. *Nuklearmedizin*. 2011;50:167–173.
- Vander Borght T, Asenbaum S, Bartenstein P, et al. EANM procedure guidelines for brain tumour imaging using labelled amino acid analogues. *Eur J Nucl Med Mol Imaging*. 2006;33:1374–1380.